

VARIATION OF TILTING STIFFNESS WITH PAD DEFORMATION IN A LARGE THRUST BEARING

D. V. SRIKANTH*, KAUSHAL K. CHATURVEDI** AND A. CHENNA KESAVA REDDY***

Abstract: The tilting pad thrust bearing is also known as the variable geometry bearing. The hydrodynamic pressure and thermal gradient induce the pad top and the flexible pivot to thermo-elastically deform. The primary objective in this paper is to optimise the deformation of the pad within the structural and thermal limits of the material. An ANSYS based finite element method is used to perform the deformation analysis. There are 8 elements in radial, 8 in circumferential and 8 along thickness to a total of 512 hexahedral Solid 226 elements in the thermo-structural deformation function. The nodal values of the elements at the bottom surface match the corresponding temperature and heat flux values of the lubrication problem. The analysis is coupled and solved in an iterative manner. Subsequently, the variation of the angular stiffness of the lubricant film with respect to the renewed film thickness resulting from pad deformation is analysed.

Keywords: finite element, structural, thermal deformation

1. INTRODUCTION

In many conventional bearing designs as in Weng Chen *et al.* (1994), factors such as the fluid temperature, viscosity, pad elastic and thermal deformations are neglected. To select thrust bearings with compatible operating conditions, characteristics such as metal temperature, load capacity, film thickness as in Hsia-Ming Chu (2007) are to be determined. In the present case to get a realistic analysis with large tilting pad thrust bearings, a numerical solution to the Reynolds' equation followed by an energy balance calculation and a thermo-elastic deformation computation are developed. Figure 1. Illustrates the geometry of the thrust pad.

A Taylor series based finite difference procedure as in Srikanth *et al.* (2009) is used to carry out the fluid dynamic analysis and determine the pressure distribution. The heat

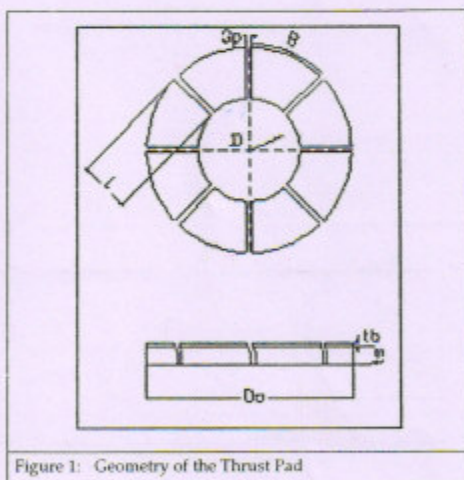


Figure 1: Geometry of the Thrust Pad

transferred as the hot lubricant is squeezed through the convergent gap causes a temperature gradient across the pad. The thermal stresses generated on account of this non-uniformity cause the deformation of the pad. This deformation is solved using an ANSYS based finite element method.

*Associate Professor in Mechanical Engineering, Bhaskar Engineering College, Yenkapally, Moinabad, R. R. District, A.P., E-mail: dsrikanth16@yahoo.com

**Senior DGM (Retired), BHEL (R & D) Vikas Nagar, Hyderabad-500093, A. P., India

***Head & Professor in Mechanical Engineering, JNTU Engineering College, Hyderabad, A.P., E-mail: drsreddy@yahoo.com

In the thermal analysis of oil films as in Ettles and Advani (1979) the advantage of limiting the analysis to two dimensions rather than three was emphasised. The two choices of considering the film in plan or elevation were examined in thrust bearings. The load capacity based on maximum allowable temperature decreased exponentially with size due to thermal distortion. It was shown in large bearings that the load capacity was progressively restricted. Thermo-elastic instability of the pad involving excessive thermal crowning caused failure.

A method for the calculation of temperature in the lubricant film of a thrust bearing was presented in Ettles (1982). This technique allowed for reverse flow and simplified calculation of hot oil carry over. An analysis to propagate thermo elastic effects in time following a change in the operating load and speed was developed.

Design of tilting pad thrust bearings on the basis of the isothermal solution of Reynolds' Equation was carried out by Chaturvedi (1984). Results of the isothermal solutions were represented by multi-nomial expressions. Performance indicators, load supported, power loss and temperature rise were calculated. Non-dimensional performance parameters and density functions for violation of constraints on film temperature and average pressure were used in the criteria function. The Nelder - mead sequential simplex algorithm based on the optimization technique was used. The program enabled the computer aided design of the tilting pad thrust bearing.

Jeng and Szeri (1986) calculated the linear stiffness and damping coefficients of pivoted pads. Both these parameters were strongly influenced by the degree of crowning. To simulate pad deformation under the combined hydrodynamic and thermal loading, spherical crowning was employed.

Gero and Ettles (1987) presented a finite element method that incorporated the temperature dependent viscosity to solve the three dimensional fluid film and pad energy equations. The systems of equations for the temperature field were solved by the iterative method. The advantage was that the parabolic or elliptic forms of the energy equation were used

with the backward differencing and up winding schemes respectively. The film and pad were treated as a single continuum and their temperatures were solved simultaneously. The transient characteristics are dependent on the slider speed and initial condition of the bearing.

Zheming and Wenkang (1993) developed a numerical solution for the compressible Reynolds' equation. It was an implicit scheme based on the Patankar-Spalding method used for solving heat transfer and fluid flow problems. The difficulties faced by various discretisation approaches in solving slider geometries with discontinuous clearances could be overcome.

Hemmi *et al.* (2005) used computational fluid dynamics software and computed the temperature distribution in the pad by solving the heat transfer in the pad, oil and interfaces simultaneously. The thermal and stress deformation were then calculated by the FEM code and used in the oil film analysis to determine the characteristics of the bearing. Comparison of the results with the experimental ones validated the computational process.

Ahmed *et al.* (2010) studied the effects of displacements of the bearing element on the fixed geometry thrust bearing performance. The TEHD study, which takes into account the local heat transfer effects and mechanical deformations of the collar and pads, was carried out on a bearing having eight pads. The influence of the runner thickness and operating conditions on the functioning of the thrust bearing were analysed. The runner thickness was found to have a very significant influence on the film thickness and the pressure field.

2. REYNOLDS' EQUATION

The following assumptions are made in the analysis.

1. Steady-state conditions exist in the oil film.
2. The lubricant is incompressible.
3. The lubricant is Newtonian.
4. Flow in the convergent wedge is laminar.
5. Pressure and shear effects on the viscosity are negligible.

6. Variation of the specific heat and density with pressure is negligible.
7. Wherever the oil film becomes divergent due to crowning or thermo-elastic distortion, cavitation is taken into account, by making pressure equal to zero, wherever its value is negative.

The Reynolds' equation is obtained by introducing the lowest order terms of the Navier Stokes equation in the continuity equation which is then integrated across the film. The Reynolds' equation in non-dimensional form is

$$\begin{aligned} & \frac{\partial^2}{\partial R^2} \left[\frac{RH^3 p}{\bar{\mu}} \right] + \frac{RH^3}{\bar{\mu}} \frac{\partial^2 P}{\partial R^2} \\ & - P \frac{\partial^2}{\partial R^2} \left[\frac{RH^3}{\bar{\mu}} \right] + \frac{1}{R\beta^2} \frac{\partial^2}{\partial \theta^2} \left[\frac{H^3 P}{\bar{\mu}} \right] \\ & + \frac{1}{R\beta^2} \frac{H^3}{\bar{\mu}} \frac{\partial^2 P}{\partial \theta^2} - \frac{P}{R\beta^2} \frac{\partial^2}{\partial \theta^2} \left[\frac{H^3}{\bar{\mu}} \right] \\ & = 12R \frac{\partial H}{\partial \theta} + 24R\beta V \end{aligned} \quad (1)$$

3. ENERGY EQUATION

Abdel-latife (1988) and Ashour (2004) considered thermo-elastohydrodynamic theories in their study. The generation of heat lowers the effective oil film viscosity and results in the decreased load capacity. The energy equation governs the heat generation and transport of oil. The energy equation for laminar flow and incompressible lubricant is given in equation (2) as

$$C_p \rho \left[q_r \frac{\partial T}{\partial r} + q_\theta \frac{1}{r} \frac{\partial T}{\partial \theta} \right] = E \quad (2)$$

Further equations (3), (4) and (5) show that

$$q_r = -\frac{h^3}{12\mu} \frac{\partial p}{\partial r} \quad (3)$$

$$q_\theta = \frac{r\omega h}{2} - \frac{h^3}{12\mu} \frac{1}{r} \frac{\partial p}{\partial \theta} \quad (4)$$

$$E = \frac{\mu}{h} (\omega r)^2 + \frac{h^3}{12\mu} \left[\left(\frac{1}{r} \frac{\partial p}{\partial \theta} \right)^2 + \left(\frac{\partial p}{\partial r} \right)^2 \right] \quad (5)$$

The Vogelpohl - Cameron equation given below in equation (6) with reference to Stachowiak (2005) shows the variation of viscosity with temperature.

$$\mu = \mu_0 e^{A/(T+B)} \quad (6)$$

It is incorporated in the iteration process.

4. STRUCTURAL DEFORMATION

The finite element used in meshing the pad model for determining the structural pad deformation is Plane 42.

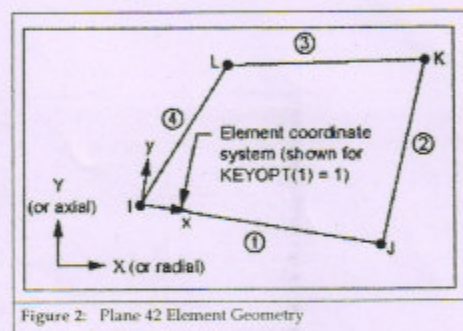


Figure 2: Plane 42 Element Geometry

The geometry, node locations, and the coordinate axis for this element are shown in the Figure 2. The element input data is for the four nodes, thickness and material properties. The orthotropic material directions correspond to the element coordinate directions. The pressures are input as surface loads on the element faces as shown by the circled numbers. Positive pressures act into the element. The inputs for the structural model are Young's modulus and Poisson's ratio of the material as given in Table 1.

5. COUPLED THERMAL-STRUCTURAL DEFORMATION

The element used to mesh the pad thermo-structural deformation model is the hexahedral Solid 226 element. The Solid 226 element has the following structural-thermal capabilities. It has up to twenty nodes with up to five degrees of freedom per node. Structural capabilities are elastic only and include large deflection and stress stiffening.

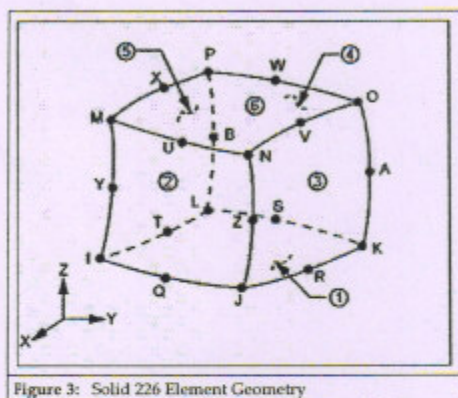


Figure 3: Solid 226 Element Geometry

Its geometry, node locations, and coordinate system are shown in the Figure 3. In both the above two types of elements the units are specified through the EMUNIT command. The nodal loading for these elements depends upon the KEYOPT (1) function value. Nodal forces are input per unit of depth for a plane analysis. The KEYOPT (1) function determines the element DOF set and corresponding force. It is set equal to the sum of the field keys. For example, KEYOPT (1) set to 11 is for a structural-thermal analysis (structural field KEY + thermal field key = 1 + 10).

6. COMPUTATIONAL PROCEDURE

The solution of the Reynolds' equation using a finite difference discretization of the thrust pad is done by considering a total of 81 nodes in the form of a grid. The finite difference equation is derived by approximating the derivatives in the differential equation via the truncated Taylor series expansion for three successive grid points. The central difference form wherein the values of the function at adjacent nodes on either side are required to evaluate the derivatives is used. The Reynolds' equation written in the finite difference form results in a set of linear algebraic equations. These equations are transformed into matrix form and solved simultaneously using available subroutines. This yields the non-dimensional pressure at each node.

Solution of the energy equation is also set up in finite differences with reference to Ettles and

Anderson (1991). The propagation method is used to solve the equation on account of its first order. The initial temperature at the leading edge is specified so that successive values of the downstream temperature are marched out in the flow direction. In this procedure, taking hot oil carry over effect into consideration the temperature distribution is obtained in a single sweep. As the energy equation (2) depends upon the pressure gradient, it is solved simultaneously with the Reynolds' equation using the same grid.

A finite element analysis of the temperature distribution, structural and coupled thermo-structural deformation of the thrust pad is done using ANSYS. In pre-processing the cross-sectional geometry, material properties and load data as given in Table 1 are input. The solid model development and the problem meshing is the first step in the analysis. For the solid model creation there are different possibilities. The ANSYS software is used in this case. The problem symmetry should be used to the extent possible

Table 1
Thrust Bearing Geometry and Properties

Description	Quantity
Outer Diameter (m)	1.275
Inner Diameter(m)	0.75
Number of Pads	6
Thickness (mm)	40
Groove width(mm)	84
Number of Springs	-
Operating Conditions	
Load (MN)	3
Rotational speed(rads/s)	14.28
Oil pot temperature(° C)	40
<i>Oil Properties</i>	
ISO grade	46
γ (cSt) at 40 ° C	73
γ (cSt) at 100 ° C	10.7
ρ (g/m ³) at 15 ° C	0.861
Pad material properties	
Mechanical Properties	
Young's modulus(GPa)	195
Poisson's ratio	0.29
Density (Kg/m ³)	7850
Thermal properties	
Thermal expansion/ C	12.2e ⁻⁶
Thermal conductivity (W/m-K at 10 C)	42.6
Specific heat (J/kg-K)	473
Heat transfer coefficient for inner surface	6.015e ⁴
Heat transfer coefficient for outer surface	30e ⁴

so as to decrease the physical dimension and use the smallest mesh-size for the given computer capacity. The model is created in ANSYS using keypoints in the axis co-ordinate system, joining consecutive lines, creating areas operating and extruding about the axis. After creation the pad model is meshed using the elements described below and simulated.

Inputs in the coupled field analysis apart from the above include thermal properties of the material including thermal conductivity, specific heat and density of the material as given in Table 1. For the plane structural deformation case, there are 8 Plane 42 elements in the radial and 8 in the circumferential direction to a total of 64 elements in the plane grid. The 3-dimensional size and shape of the plane 42 element grid is visible by switching on the display and the element function.

For the coupled thermo-structural deformation the elemental plot of the pad is displayed in Figure 4. There are 8 elements in radial, 8 in circumferential and 8 along thickness to a total of 512 hexahedral Solid 226 elements in the deformation function.

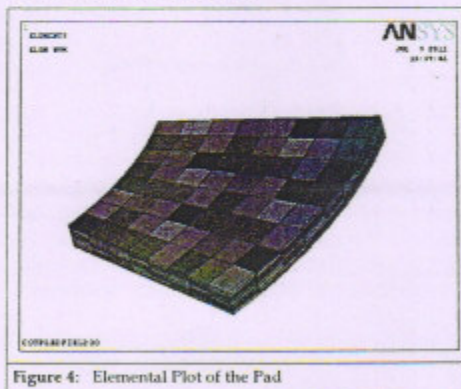


Figure 4: Elemental Plot of the Pad

Using the axis symmetric boundary condition pressure and corresponding structural load are applied on the area A2 at the bottom surface of pad as per Figure 5.

2) The convection from the areas A1, A5, A4 and A6 as shown in Figure 5 where in the bulk temperature is 40 C and convection film coefficient value is 4e6 is considered.

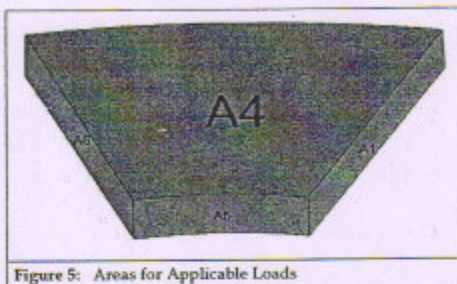


Figure 5: Areas for Applicable Loads

(3) The heat flux values for the elemental nodes of the bottom surface of the pad are obtained from the solution of the energy equation.

(4) Radiation heat transfer from the pad is not considered.

To view results for deformation the current load system functions of plot results, counter plot nodal solution and displacement vector are chosen.

7. TILTING STIFFNESS

Figure 6 shows two different pad tilt positions 1 & 2 and corresponding film shapes for which torques are calculated. Referring to Figure 7 we have the initial value of a in equation (7) as

$$a = \frac{h_1}{h_2} - 1 \quad (7)$$

For the case under consideration the value of h_1 is constant and h_2 is varied by 20%, 15%, 10%, 7%, 5%, 2%, 1%, 0.5% respectively. The corresponding values of ' a ' are calculated using the formula in equations (8) and (9).

$$a = \frac{(ah_1 + h_2 \Delta h_0)}{h_2 - h_1 \Delta h_0} \quad (8)$$

$$a = \frac{(a + \Delta h_0)}{1 - \Delta h_0} \quad (9)$$

where $\Delta h_2 = \% \text{ of } h_2 \text{ increased at leading edge.}$

The tilting stiffness of the film pertaining to the 2-1 pair are calculated as follows. For each variation of h_2 , the following values are calculated. X is the x-coordinate of the centre of pressure of the film shape under consideration.

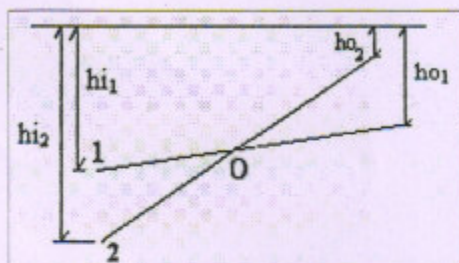


Figure 6: Pad Showing 1, 2 Positions for Torque Calculation

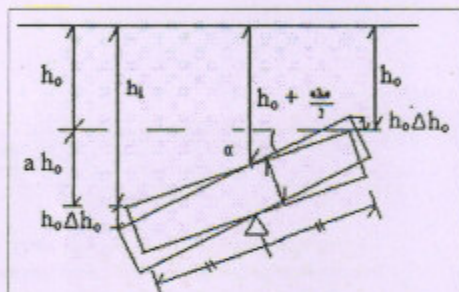


Figure 7: Pad Showing Inlet and Outlet Film Thickness

$$B = R_{\sigma} \times \beta$$

$X = r \sin(\theta - \theta_{\sigma})$ to obtain K_T in equation (10)

$$KT_1 = \frac{W_1 X B}{a(h_{s2} - h_{s1})} \quad (10)$$

Substituting as per equation (11) load capacity

$$W^* = \left[\frac{h_0^3}{BL^2 U \mu_{eff}} \right] \quad (11)$$

in place of W in the following equation (12) with reference to Ettles (1991)

$$K_T = \frac{WXB}{ah_0} \quad (12)$$

By rationalising the non-dimensional angular stiffness K_T^* of the film to a dimensionless number we obtain it in equation (13) as

$$K_T^* = K_T \left[\frac{h_0^2}{B^2 L^2 U \mu_{eff}} \right] \quad (13)$$

8. RESULTS AND DISCUSSIONS

In the plane structural analysis the deformation for the parameters is $0.726e^{-3}$ and the distribution is as in Figure 8.

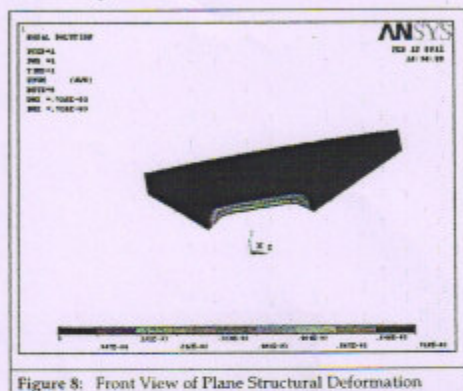


Figure 8: Front View of Plane Structural Deformation

The plan view of the plane structural deformation distribution with maximum and minimum regions is as shown in Figure 9.

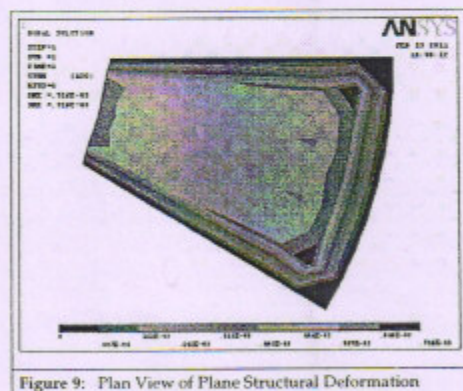


Figure 9: Plan View of Plane Structural Deformation

The thermal loads are calculated as per the temperature distribution diagram shown in Figure 10 below and the maximum temperature is at the top right corner of the trailing edge.

In the coupled field analysis the deformation is $0.7043e^{-3}$. The maximum and minimum values are $0.130e^{-3}$ and $0.31e^{-4}$ and the regions are as in Figure 11.

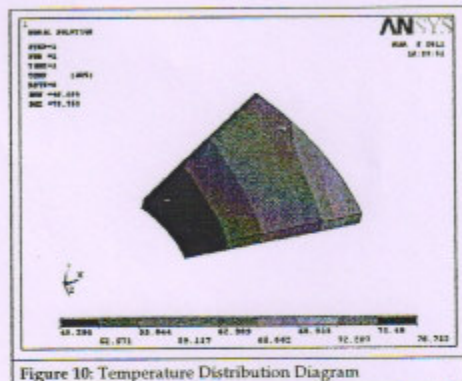


Figure 10: Temperature Distribution Diagram

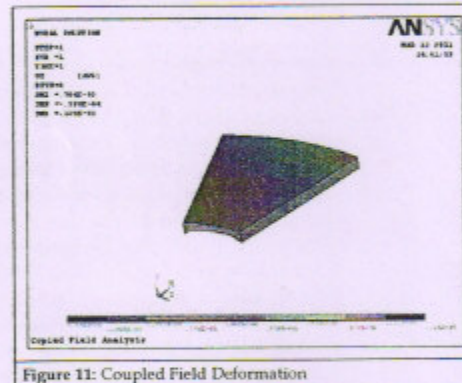


Figure 11: Coupled Field Deformation

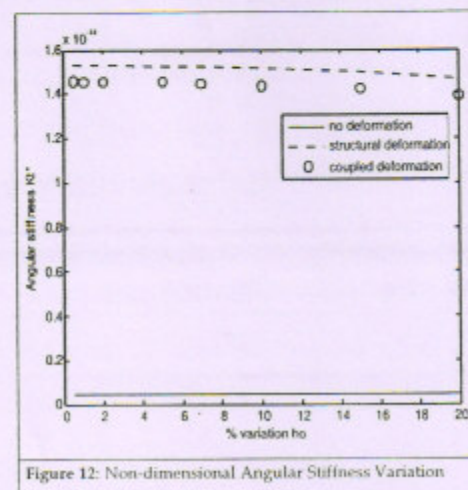


Figure 12: Non-dimensional Angular Stiffness Variation

Figure 12 clearly shows the variation of non dimensional angular stiffness with the type of pad deformation for increasing percentage variation of film thickness. There is a big difference in K_T^* values between a pad which does not take deformation into consideration and one which has either plane structural or coupled thermo-structural deformation. This underlies the importance of pad deformation in large hydro generator thrust bearings. The difference between angular stiffness values between the two types of deformations considered is not large and the structural deformation produced marginally higher K_T^* values than the coupled field deformation.

9. CONCLUSIONS

Reynolds' equation is modified and a finite difference based solution procedure for finding pressure values is written and verified. Numerical integration to these pressure points gives the load. The viscosity variations and corresponding temperature distribution in the transport of the lubricant are taken into consideration for the determination of the film tilting stiffness coefficients. Solving the Reynolds' equation and accounting for all the factors which influence the performance characteristics is a very involved procedure. The plane structural and coupled thermo-structural deformation of the pad were simulated and studied. Fast computational routines are developed to evaluate the angular stiffness coefficients. Torques and oil film shape parameters, for h_0 variation from 0.5-20% for the 2-1 pair are calculated. The governing equations for angular stiffness pertaining to the 2-1 pair are formulated and verified. The value of K_T^* converge asymptotically as the % h_0 increases from 0.5 to 20%. The importance of taking pad deformations in consideration for large thrust bearings was verified.

References

- [1] Weng Jeng Chen, Zeidan, F.Y. and Jain, D., (1994), "Design Analysis and Testing of High Performance Bearings in a High Speed Integrally Geared Compressor, Proceedings of the Twenty third Turbo Machinery Symposium, Texas A&M University, USA.
- [2] Hsia-Ming Chu, (2007), "Shape Optimum Design of Slider Bearings using Inverse Methods," *Tribology International*, 40, 906-914.

- [3] Srikanth, D. V., Chaturvedi, K. K., Reddy, A. C. (2009), "Theoretical Predictions and Comparison of Oil Film Thickness, Pressure and Dynamic Characteristics of a Tilting Pad Thrust Bearing in Large Vertical Machines", *Indian Journal of Tribology*, 4, 2, 30-37.
- [4] Ettles, C. M. M. and Advani, S. (1979), "The Control of Thermal and Elastic Effects in Thrust Bearings", Proceedings of the 6th Leeds-Lyon Symposium on Tribology, 105-116.
- [5] Ettles, C. M. M. (1982), "Transient Thermo Elastic Effects in Fluid Film Bearings", *Wear*, 79, 53-71.
- [6] Chaturvedi, K. K. (1984), "Computer Program for Optimization of Tilting Pad Thrust Bearing Design for CAD Application", National Conference on Industrial Tribology, July, Hyderabad, pp. 141-148.
- [7] Jeng M., C. and Szeri A., Z. (1986), "A Thermo-hydrodynamic Solution of Pivoted Thrust Pads: Part III - Linearized Force Coefficients", *Transactions of the ASME, Journal of Tribology*, 108(2), 214-218.
- [8] Gero L. R., and Ettles C. M. M. (1987), "A Three Dimensional Thermo- hydrodynamic Finite Element Scheme for Fluid Film Bearings", *STLE Tribology Transactions*, 31, 2, 182-191.
- [9] Zheming, Z. and Wenkang, S. (1993), "A New Method for the Numerical Solution of the Reynolds' Equation at Low Spacing", *Transactions of the ASME, Journal of Tribology*, 115(1), 83-87.
- [10] Hemmi, M., Hagiya, K., Ichisawa, K. and Fujita S. (2005), "Computation of Thermal Deformation of Thrust Bearing Pad Concerning the Convection by Non-Uniform Oil Flow", World Tribology Congress III, September 2005, Washington D.C, pp. 61-62.
- [11] Ahmed, S. A., Fillon, M. and Maspeyrot, M. (2010), "Influence of Pad and Runner Mechanical Deformations on the Performance of a Hydrodynamic Fixed Geometry Thrust Bearing" Proceedings of the Institution of Mechanical Engineers, Part J: *Journal of Engineering Tribology*, 224(4), 305-315.
- [12] Abdel-latif L. A. (1988), "Analysis of Heavy Loaded Tilted Pads Thrust Bearings with Large Dimensions under TEHD Condition", *ASME Journal of Tribology*, 110, 407-476.
- [13] Ashour N. M., and El-Butch A. (2004), "Prediction of the Thermal Characteristics of Thrust Bearing with Arbitrarily Pivoted Pad", International Colloquium tribology Stuttgart-Ostfildern, Germany, January 13-16.
- [14] Stachowiak G. W., and Batchelor A. W. (2005), "Engineering Tribology", Elsevier, Third Edition, 13-14.
- [15] Ettles, C. M. M. and Anderson, H. G. (1991), "Three - Dimensional Thermo - Elastic Solutions of Thrust Bearings using Code Marmac 1", *ASME Transactions, Journal of Tribology*, 112, 405- 412.
- [16] Ettles, C. M. M. (1991), "Some Factors Affecting the Design of Spring Supported. Thrust Bearings in Hydroelectric Generators", *ASME Trans., Journal of Tribology*, 113, 626-632.